Temperature-driven phase transformation in self-assembled diphenylalanine peptide nanotubes

FAST TRACK COMMUNICATION

Temperature-driven phase transformation in self-assembled diphenylalanine peptide nanotubes

A Heredia[1]**, I Bdikin**[2]**, S Kopyl**[2]**, E Mishina**[3]**, S Semin**[3]**, A Sigov**[3]**,
K German**[4]**, V Bystrov**[1,5]**, J Gracio**[2] **and A L Kholkin**[1]

[1] Department of Ceramics and Glass Engineering and CICECO, University of Aveiro,
3810-193 Aveiro, Portugal
[2] Centre for Mechanical Technology and Automation (TEMA), University of Aveiro,
3810-193 Aveiro, Portugal
[3] Moscow State Institute of Radioengineering, Electronics and Automation, 119454 Moscow, Russia
[4] Institute of Applied Physics, Kishinev, MD-2028, Republic of Moldova
[5] Institute of Mathematical Problems of Biology, Puschino, Moscow District, Russia

E-mail: kholkin@ua.pt

Abstract

Diphenylalanine (FF) peptide nanotubes (PNTs) represent a unique class of self-assembled functional biomaterials owing to a wide range of useful properties including nanostructural variability, mechanical rigidity and chemical stability. In addition, strong piezoelectric activity has recently been observed paving the way to their use as nanoscale sensors and actuators. In this work, we fabricated both horizontal and vertical FF PNTs and examined their optical second harmonic generation and local piezoresponse as a function of temperature. The measurements show a gradual decrease in polarization with increasing temperature accompanied by an irreversible phase transition into another crystalline phase at about 140–150 °C. The results are corroborated by the molecular dynamic simulations predicting an order–disorder phase transition into a centrosymmetric (possibly, orthorhombic) phase with antiparallel polarization orientation in neighbouring FF rings. Partial piezoresponse hysteresis indicates incomplete polarization switching due to the high coercive field in FF PNTs.

S Online supplementary data available from stacks.iop.org/JPhysD/43/462001/mmedia

(Some figures in this article are in colour only in the electronic version)

1. Introduction

Piezoelectricity is the ability of crystalline materials without a centre of inversion to produce mechanical stress/strain under an electric field or charge/voltage under a mechanical force. This property is widely used nowadays in many applications including acoustic transducers, sensors/actuators, piezomotors, accelerometers and gyroscopes, just to name a few [1]. Following current trends for miniaturization,

piezoelectric materials have been suggested to be the key elements of future micro- and nanoelectromechanical systems (MEMS and NEMS), where piezoelectric effect offers many advantages over electrostatic actuation [2, 3]. In view of growing interest in biomedical applications, bio-organic materials having significant piezoactivity (in particular, ferroelectrics [4]) are required for further progress in the design of modern piezo-MEMS and NEMS. Several biologically originated materials were identified to be piezoelectric but
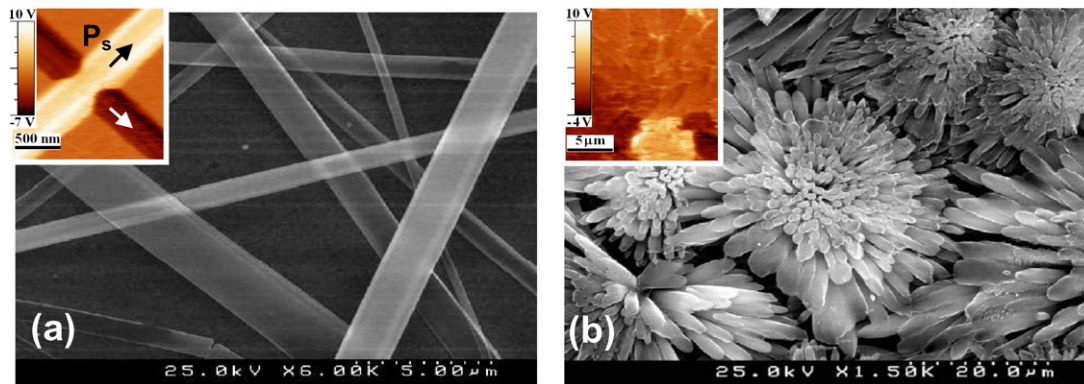
IOP FTC ▶▶▶

J. Phys. D: Appl. Phys. 43 (2010) 462001   Fast Track Communication

Figure 1. Representative SEM images of horizontal (*a*) and vertical (*b*) PNTs deposited from the solution. The insets show the representative PFM in-plane (*a*) and out-of-plane (*b*) contrasts. PFM measurements on vertical tubes were actually performed on agglomerated tubes where scanning in contact mode was only possible.

their piezoelectric properties were rather weak to be used in applications [5, 6]. Another challenge is to fabricate nanostructural materials such as nanotubes for the activation of piezoelectricity on the nanoscale [7]. Recently, strong piezoelectricity (of the order of that in the classical transducer material $LiNbO_3$) has been discovered in bio-inspired peptide nanotubes (PNTs) made by a self-assembly process of small diphenylalanine, NH_2–Phe–Phe–COOH (FF), peptide monomers [8]. These PNTs have first been discovered from the determination of the smallest recognition motif of the amyloid-β protein, associated with over 30 diseases, mostly neurodegenerative ones such as Alzheimer's, Huntington's, Parkinson's, Creutzfeldt–Jacob and prions, but also sclerosis (Lou Gehrig's disease) and type-II diabetes [9]. They are made from amino acids, self-assembled in unique stable tubes with hydrophilic hollows [10], having high Young's modulus and chemical stability [11]. X-ray and electron diffraction studies have revealed that their room temperature crystal structure is compatible with the space group $P6_1$ [12], allowing many physical phenomena described by the odd-rank tensor, including optical second harmonics generation, pyroelectricity, linear electro-optic effect and piezoelectricity. Crucial for applications is the temperature dependence of polarization in FF PNTs, and the possible phase transformation under heating above room temperature. In this work, we present our recent findings on the temperature-dependent polarization response in FF PNTs, studied via piezoresponse force microscopy (PFM) [13] and optical SHG.

Second harmonic generation (SHG) is known to be an efficient tool for studying different types of phase transitions, such as surface reconstruction of the collagen 3D configuration in teeth [14], laser-induced melting [15], phase transitions in molecular monolayers [16] and structural phase transition at the surface [17]. In ferroelectrics, diagnostics with SHG is based on the sensitivity of SHG intensity to the order parameter; therefore, the temperature dependence of the square root of SHG intensity typically follows the polarization behaviour. In this way, various phase transitions in classical ferroelectrics [18] as well as in organic materials [19] were successfully identified. In organic materials, SHG is also sensitive to conformational transitions, including irreversible transformations [20]. The aim of this work was thus to

study temperature-dependent SHG and PFM, with the focus on possible phase transitions and ferroelectricity in this material.

2. Experimental details

FF PNTs were self-assembled by dissolving the FF dipeptide in the lyophilized form (Bachem, Switzerland) in 1,1,1,3,3,3-hexafluoro-2-propanol at a stock concentration of $100\,mg\,ml^{-1}$. For horizontal tubes, $2\,\mu l$ of the stock solution was diluted with $98\,\mu l$ of dd-H_2O. The diluted solution was deposited onto Au- or Pt-coated silicon substrates and left overnight for drying. For vertical tubes, $30\,\mu l$ of the stock solution was cast directly on a substrate with an area of $\approx 2\,cm^2$ and left for complete evaporation for 12 h [21]. The local piezoresponse measurements were performed with a commercial AFM (Ntegra Prima, NT-MDT) equipped with an external function generator and a lock-in amplifier as already described elsewhere [8]. We used doped Si cantilevers with spring constants of 0.5–$1\,N\,m^{-1}$. Ac voltage of 2 V amplitude and frequency 5 kHz was applied to the counter electrode while the tip was grounded. For the SHG measurements, the beam of a Ti : sapphire laser (790 nm with a pulse width of about 100 fs, a repetition rate of 80 MHz and an average power of 15 mW) was focused onto a spot of about $50\,\mu m$ diameter. Reflection geometry was used at a $45°$ incidence. Both fundamental and SHG waves were polarized with the electric field vector in the incidence plane (p-in, p-out). The SHG signal at 380 nm was filtered by a colour filter (BG39) and detected by a photomultiplier tube in photon counting mode. SHG images filtered by BG39 were taken with a CCD camera using an optical microscope (magnification ×45) under femtosecond laser irradiation. The CCD camera was then mechanically scanned to acquire the SHG image with the resolution of a few micrometres.

3. Results and discussion

Figure 1 shows the representative SEM and PFM images of the fabricated PNTs assembled horizontally and vertically on metallized substrates as described above. A variety of tubes of different lengths, diameters and orientations were
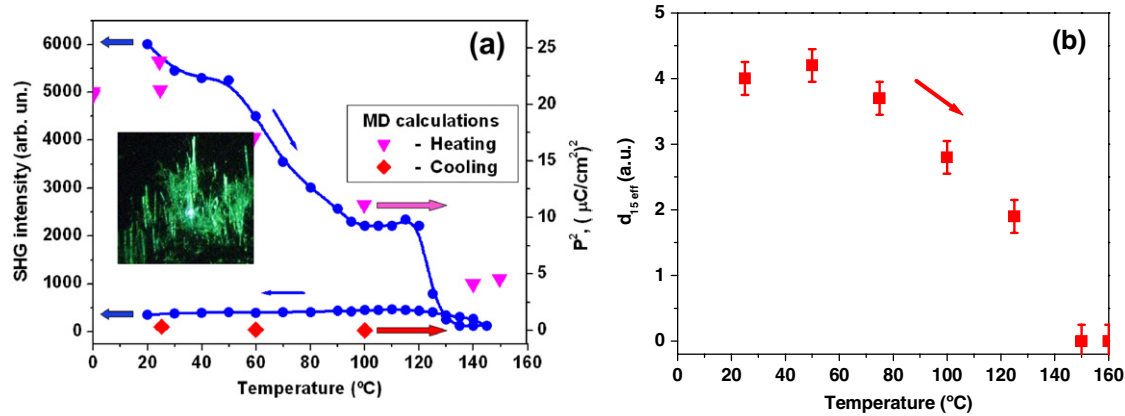
J. Phys. D: Appl. Phys. **43** (2010) 462001

IOP FTC ▶▶▶

Fast Track Communication

Figure 2. Temperature dependences of SHG (*a*) and PFM signals (*b*) for FF PNTs. The data points on SHG curves are compared with the MD calculations undertaken for parallel double-stacked FF in the hexagonal phase (triangles) and antiparallel ones in the orthorhombic phase (diamonds).

observed. A strong piezoelectric contrast was observed on both horizontal (via lateral PFM signal, inset to figure 1(*a*)) and vertical tube assemblies (via vertical PFM, inset to figure 1(*b*)). These results confirm the already published data [8] on horizontal tubes where only the shear piezoelectric coefficient ($d_{15} \sim 60$ pm V^{-1} on sufficiently big tubes) could be measured. The estimate of the effective longitudinal piezoelectric coefficient d_{33} in vertical tubes yields values in excess of 30 pm V^{-1}, i.e. it exceeded that for LiNbO$_3$ [22]. Figure 2(*a*) represents the variation of the average shear PFM contrast with increasing temperature measured on horizontal tubes. The contrast gradually decreases with temperature demonstrating monotonic d_{15} dependence and ultimate disappearance of piezoresponse at a temperature of ~150 °C. It should be noted that the contrast becomes irreversible if the sample is heated above 100 °C, i.e. it is not recovered after cooling down to room temperature and remains practically zero after heating up to 140–150 °C. This hints to the possible phase transformation to another phase on heating, as no visible degradation of the topography was found. Figure 2(*b*) shows the temperature dependence of SHG intensity measured on vertical tubes (both heating and cooling runs). The results are, in general, consistent with the temperature-dependent PFM contrast measurements; however, many more details were observed on the temperature curve. A clear cusp on the SHG intensity curve at about 50 °C is followed by a significant reduction in the intensity until a plateau between 100 and 120 °C is reached. Finally, the SHG signal drops down at ~130 °C (irreversibly as evidenced by the cooling curve). It should be noted that these data are consistent with the recent studies of thermal stability of PNTs via differential thermal gravimetry (DTG) [23]. These measurements revealed that FF PNTs exhibit a clear weight loss at temperatures close to ~50 °C (anomaly seen also with SHG, figure 2(*b*)) and at ~140 °C. The rearrangement of the crystalline structure of PNTs at 50 °C (as evidenced by the anomaly of the SHG signal) can be due to the phase transition between two piezoelectric phases as confirmed by the existence of piezoresponse, both below and above this temperature (figure 2(*a*)). Details of this phase transition are outside the scope of this paper and will be reported elsewhere. In general,
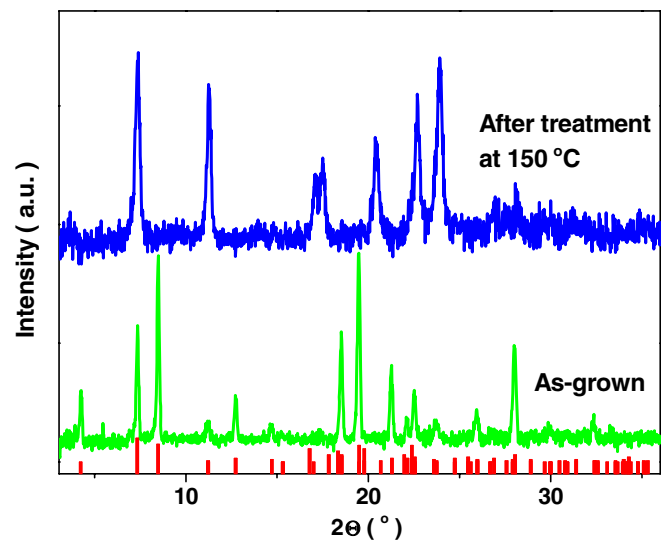

Figure 3. X-ray diffraction spectra of FF PNTs before and after annealing at 150 °C for 1 h. Vertical bars are generated using structural data from the CCDC file no 163340.

the apparent decrease in the piezoelectric contrast and SHG intensity (figure 2) with temperature is a clear signature of the irreversible phase transformation to a high-symmetry phase as often observed in molecular crystals [24, 25].

Figure 3 shows the typical x-ray diffraction patterns of the studied vertical PNTs before and after temperature annealing at 150 °C for 1 h. In virgin samples (grown at room temperature) all observed peaks correspond to the expected hexagonal structure already reported for FF PNTs ($a = 24.071$ Å, $c = 5.456$ Å, $\alpha = 120°$, space group $P6_1$) [12]. The diffraction peaks for annealed PNTs are apparently different, belonging to another crystalline phase. All diffraction peaks after annealing could be explained based on the appearance of an orthorhombic structure with the unit cell parameters $a = 5.210$ Å, $b = 24.147$ Å, $c = 41.072$ Å (see table 1 (stacks.iop.org/JPhysD/43/000000/mmedia) of supplementary material for more details). The possible phase transition between hexagonal and orthorhombic phases upon annealing is illustrated in figures 4(*b*) and (*c*), where it is shown how

J. Phys. D: Appl. Phys. **43** (2010) 462001

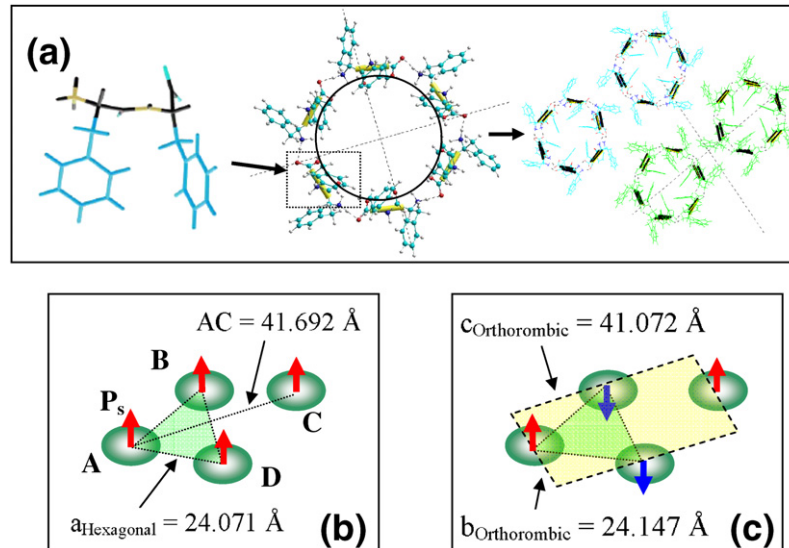**IOP** FTC ▶▶▶

Fast Track Communication

Figure 4. (*a*) Schematic illustration of the self-assembly process of PNTs: from individual FF monomer molecules to six dipeptides (6FF) forming a ring and finally to whole structure of PNTs. Models of the hexagonal (*b*) and orthorhombic (*c*) structures of PNTs (detailed explanation is given in the text).

the initial hexagonal unit cell could be transformed into the orthorhombic one via a small deformation of the FF rings. The mainframe of the FF PNT structure consists of the FF rings (figure 4(*a*)), formed from six individual FF molecules (6FF), in accordance with [12]. Each ring possesses a dipole moment P_s along the tubular *OZ*-axis perpendicular to the ring plane and forms the hexagonal structure [12] from four rings (figure 4(*a*), right). It is suggested that for the hexagonal structure all 6FF rings (A, B, C and D) have the same orientation as the individual P_s (figure 4(*b*)), this being compatible with the total large dipole moment and strong piezoresponse in PNTs grown at room temperature [8]. Antiparallel orientation of P_s for the neighbouring 6FF rings (A and C opposite to B and D) produces a novel orthorhombic structure with zero total polarization (figure 4(*c*)) for annealed tubes.

To understand further the molecular structure of the FF PNTs and the possible mechanisms of their self-assembly and phase transitions, we performed molecular modelling and molecular dynamic (MD) simulations using HypeChem 7.52 [26]. The isolated ring with six dipeptides as well as the parallel stacking of two rings (see figure S1 (stacks.iop.org/JPhysD/43/000000/mmedia) of supplementary material) were studied by the geometry optimization of the total energy and MD runs using molecular mechanics (MM) methods (BIO CHARM) in combination with a first-principles quantum approach (*ab initio* and PM3 semi-empirical). It was found that 6FF forms ordered rings (hexagonal structure, $P6_1$) with inner and outer diameters of $\sim$10.5 Å and 25 Å, respectively, connected by N–H...O hydrogen bonds with O–H lengths of $\sim$1.65 Å. This is in full agreement with the results of [12]. Further, we calculated the dipole moment being $\sim$1.3 Debye for a single 6FF ring, directed along the *OZ* hexagonal axis corresponding to a spontaneous polarization $P \approx 0.24\,\mu$C cm^{-2}. These data also correspond to the reported values for isolated FF units [12] (figure 4(*a*)). Figure S1 represents the model of parallel double-stacked

6FF units. In this case, the optimization with BIO CHARM (after PM3 calculations) leads to a large dipole moment $D_t \sim 42$ Debye ($P \sim 4.0\,\mu$C cm^{-2}). After additional PM3 semi-empirical optimization it further increases up to $D_t \sim 52$ Debye and the estimated polarization value reaches $\sim$5 μC cm^{-2}. On the basis of this model we performed MD runs and simulations at different temperatures. The result is fully consistent with the experimentally obtained SHG and PFM data, i.e. the average dipole moment gradually decreases as a function of temperature (cf calculations with experimental data in figure 2(*b*)). The polarization is about 5 μC cm^{-2} at 25 °C and decreases to $\sim$2 μC cm^{-2} at 100 °C. The results for a parallel stacked FF ring model correspond to the hexagonal phase and the experimentally observed large dipole moment and high piezoelectric coefficient in virgin structures, while the antiparallel orientation of neighbouring tubes corresponds to the orthorhombic phase with a very small total dipole moment, as shown in figure 2(*b*). Moreover, this result made us believe that the dipole ordering along the *OZ* hexagonal axis for the hexagonal phase is due to a cooperative dipole effect (as common to ferroelectric systems, while the orthorhombic phase is similar to antiferroelectrics), and polarization switching is possible if a high-enough electric field is applied along this axis.

Following this idea, we attempted to measure piezoresponse hysteresis on virgin (not annealed) vertical PNTs. The simulation data have led us to the conclusion that the corresponding coercive field would be very high, in the order of $\sim$30 MV cm^{-1}, and has an asymmetric character as a result of the strong internal bias field. This prediction is fully consistent with the experimental result (figure 5) where a hysteretic-like dependence of the effective d_{33} versus applied bias is obvious. However, the loop reveals partial switching of the polarization along the hexagonal axis with superimposed linear behaviour that could be caused by the electrostatic contribution to the piezoresponse (Maxwell stress) [27]. Taking
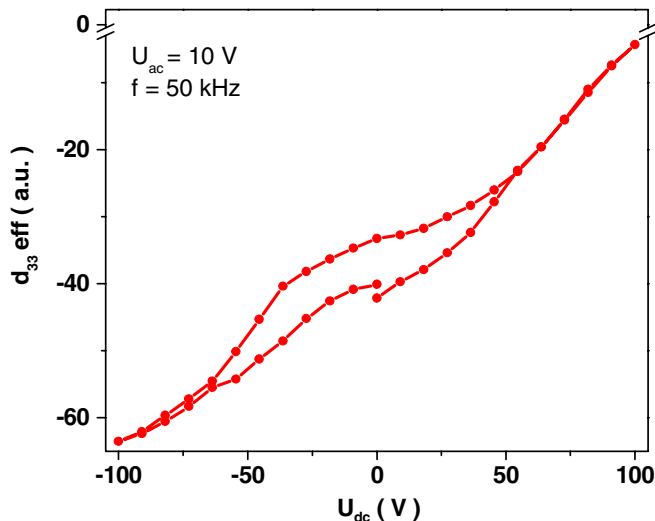
J. Phys. D: Appl. Phys. **43** (2010) 462001

IOP FTC ▶▶▶

Fast Track Communication

Figure 5. Out-of-plane piezoresponse hysteresis taken on vertical PNTs. The piezoresponse signal does not change sign even at a maximum bias due to the high coercive field of the hexagonal structure.

into account some flexibility of the PNTs at the contact point, and apparent non-local electrostatic interaction, this possibility cannot be ruled out. The results are in line with the recent piezoresponse measurements in PZT nanotubes where a similar character of the piezoresponse hysteresis was found [28]. This signifies that the local measurements in such complex geometries can be overshadowed by spurious signals irrespective of the nature of the material. The polarization offset observed in the hysteresis loops (figure 5) could be due to the fact that the available electric field is insufficient for switching, and only a small reverse domain (unstable with time) is formed under a maximum bias. This is confirmed by the absence of any switched polarization after the consequent PFM imaging. Since the available electric field by the tip is quite low (in the first approximation ∼100–200 kV cm^{-1} under the bias 10 V), this reduces the opportunities for using vertical FF PNTs as media for high-density data storage. Unfortunately, higher biases destroy the tubes. Molecular simulations made under an electric field were in line with the experimental observation (table 3 (stacks.iop.org/JPhysD/43/000000/mmedia) of supplementary material) and showed that an antiparallel field of about 5 MV cm^{-1} is only able to decrease the polarization value by about 12%.

Another important result of our simulations is the tentative explanation of the observed hexagonal–orthorhombic irreversible transformation, because the calculations show that the temperature increase leads to strong changes in the condensation energies, particularly in modifying inter-tube interaction. The approach for the inter-tube interaction calculations with distances and determination of the condensation energies is similar to that used in [29]. As a result, the inter-tube condensation energy decreases with temperature and, at a temperature of about 150 °C, it becomes comparable to thermal energy kT (figure S1, table 2 (stacks.iop.org/JPhysD/43/000000/mmedia) of supplementary material). This ultimately leads to the dissociation of PNT tubes and reorganization of their structure, so that the

antiparallel orientation of the rings becomes energetically favourable at a high-enough temperature. All in all, the predicted re-orientation of polar molecular dipole groups in neighbouring FF tubes leads to the compensation of the total polarization to almost zero value, accompanied by a symmetry change and increase in the unit cell size (see, for illustration, figures 4 and S1 and tables 1 and 2 of supplementary material). We believe that for FF PNTs prepared at room temperature, the parallel orientation of the polar moments related to individual nanotubes is energetically favourable; while at $T \geqslant 150$ °C the preferred conformation is antiparallel leading to a doubling of the unit cell. This model is in line with the experimental XRD results (figure 3) and the orthorhombic structure shown in figure 4. Upon cooling this phase persists down to room temperature, being metastable within the extended period of time. The calculated transition temperature is close to that observed by PFM and SHG experiments. AFM and SEM data (figure S2 (stacks.iop.org/JPhysD/43/000000/mmedia) of supplementary material) indicate notable degradation of the tube surface consistent with earlier reports [30].

It is already well known that FF peptides can form various supra-molecular structures. One of the most studied conformations is a hexagonal molecular nanotube structure, similar to that observed in liquid crystals (LC) [31, 32]. From this point of view it is evident that the studied PNTs could be considered as an analogue of a smectic C* (SmC*) phase, composed of six FF L-chiral molecules arranged as a single 6FF stable ring (one smectic disc further forms a discotic-like columnar structure [24, 33]). Obviously, such a molecular LC is prone to polymorphic transformations [25] that occur due to a very wide variation of the peptide's bond torsion angle. Some of these polymorphic phases could be metastable leading to possible irreversible phase transitions. It is worth noting that structural polymorphism exists in the amyloid fibrils related to PNTs [34]. Similar transitions were observed in the temperature dependence of LC lipid systems [35] and in DNAs that change from the tubular hexagonal to orthorhombic structure [36]. It is clear that our results resemble the well-known phase transition in LCs from the ferroelectric-like SmC* to paraelectric SmA phase. Details of the molecular simulations and calculations of the condensation energies are reserved for a future publication.

4. Conclusions

In conclusion, our measurements revealed an important feature of the polarization behaviour in self-assembled FF PNTs. As confirmed by the PFM and SHG measurements, the polarization gradually decreases from room temperature to 140 °C, and experiences an irreversible phase transformation to another (probably orthorhombic) crystalline phase with zero polarization. This phase persists upon cooling to room temperature. Partial polarization switching is observed by the application of a strong electric bias to the PFM tip, but full switching is impossible due to the high coercive field. This result is in line with the fact that ferroelectric-like behaviour has originated from hydrogen bonds among the FF monomers, which break upon the temperature increase.

J. Phys. D: Appl. Phys. **43** (2010) 462001

IOP FTC ▶▶▶

Fast Track Communication

This transformation is extremely important in view of the foreseeable applications of PNTs as sensors and actuators.

Acknowledgments

References

[1] Safari A and Akdogan K (ed) 2008 *Piezoelectric and Acoustic Materials for Transducer Applications* (New York: Springer)
[2] Polla D L and Francis L F 2006 *MRS Bull.* **21** 34
[3] Muralt P 2008 *J. Am. Ceram. Soc.* **91** 1385
[4] Horiuchi S and Tokura Y 2008 *Nature Mater.* **7** 357
[5] Fukada E and Yasuda I 1957 *J. Phys. Soc. Japan* **12** 1158
[6] Halperin C, Mutchnik S, Agronin A, Molotskii M, Urenski P, Salai M and Rosenman G 2004 *Nano Lett.* **4** 1253
    Rodriguez B J, Kalinin S V, Shin J, Jesse S, Grichko V, Thundat T, Baddorf A P and Gruverman A 2006 *J. Struct. Biol.* **153** 151
[7] Wang Z L 2007 *Mater. Today* **10** 20
[8] Kholkin A L, Amdursky N, Bdikin I, Gazit E and Rosenman G 2010 *ACS Nano* **4** 610
[9] Harkany T, Hortobágyi T, Sasvári M, Kónya C, Penke B, Luiten P G M and Nyakas C 1999 *Prog. Neuropsychopharmacol. Biol. Psychiatry* **23** 963
[10] Reches M and Gazit E 2003 *Science* **300** 625
[11] Kol N, Adler-Abramovich L, Barlam D, Shneck R Z, Gazit E and Rousso I 2005 *Nano Lett.* **5** 1343
[12] Görbitz C H 2001 *Chem. Eur. J.* **7** 5153
[13] Bonnell D A, Kalinin S V, Kholkin A L and Gruverman A 2009 *MRS Bull.* **34** 648
    Kalinin S V, Setter N and Kholkin A L 2008 *MRS Bull.* **34** 634
[14] Hoefer U, Li L, Ratzlaff G A and Heinz T F 1995 *Phys. Rev.* B **52** 5264
[15] Shank C V, Yen R and Hirlimann S 1983 *Phys. Rev. Lett.* **51** 900
[16] Rasing Th, Shen Y R, Kim M W and Grubb S 1985 *Phys. Rev. Lett.* **55** 2903
[17] Mishina E D, Misuryaev T V, Sherstyuk N E, Lemanov V V, Morozov A I, Sigov A S and Rasing Th 2000 *Phys. Rev. Lett.* **85** 3664
[18] Aktsipetrov O A, Apukhtina S A, Nikulin A A, Vorotilov K A, Mishina E D and Sigov A S 1991 *JETP Lett.* **54** 563
[19] Aktsipetrov O A, Misuryaev T V, Murzina T V, Blinov L M, Fridkin V M and Palto S P 2000 *Opt. Lett.* **25** 411
[20] Theodossiou T A, Thrasivoulou C, Ekwobi C and Becker D L 2006 *Biophys. J.* **91** 4665
[21] Reches M and Gazit E 2006 *Nature Nanotechnol.* **1** 195
[22] Landolt H and Bornstein R 1981 *Numerical Data and Functional Relationships in Science and Technology* (New Series) vol III/16 (Berlin: Springer)
[23] Adler-Abramovich L, Reches M, Sedman V L, Allen S, Tendler S J B and Gazit E 2006 *Langmuir* **22** 1313
[24] deGennes P G and Prost J 1993 *The Physics of Liquid Crystals* (Oxford: Clarendon)
[25] Bernstein J 2002 *Polymorphism in Molecular Crystals* (Oxford: Clarendon)
[26] 2002 HyperChem.7.52. *Tools for Molecular Modeling* Hypercube, Inc.
[27] Hong S, Woo J, Shin H, Jeon J U, Pak Y E, Colla E L, Setter N, Kim E and No K 2001 *J. Appl. Phys.* **89** 1377
[28] Scott J F *et al* 2008 *Nano Lett.* **8** 4404
[29] Nakanishi T, Okamoto H, Nagai Y and Takeda K 2002 *Phys. Rev.* B **66** 165417
[30] Sedman V L, Adler-Abramovich L, Allen S, Gazit E and Tendler S J B 2006 *J. Am. Chem. Soc.* **128** 6903
[31] Scanlon S and Aggeli A 2008 *Nano Today* **3** 22
[32] Yan X, Zhua P and Li J 2010 *Chem. Soc. Lett.* **39** 1861
[33] Saez I M and Goodby J W 2005 *J. Mater. Chem.* **15** 26
[34] Fandrich M, Meinhardt J and Grigorieff N 2009 *Prion* **3** 89
[35] Raudenkolba S, Wartewigb S and Neuberta R H H 2005 *Chem. Phys. Lipids* **133** 89
[36] Livolant F, Leforestier A, Durand D and Doucet J 1993 *Lect. Notes Phys.* **415** 33